Article

Not peer-reviewed version

Chromosomal Location and Identification of TBX20 as a New Gene Responsible for Familial Bicuspid Aortic Valve

Yan-Jie Li , Su Zou , Yi-Zhe Bian , Xing-Yuan Liu , Chen-Xi Yang , Li Li , Xing-Biao Qiu , Ying-Jia Xu , Yi-Qing Yang *, Ri-Tai Huang *

Posted Date: 18 February 2025

doi: 10.20944/preprints202502.1131.v1

Keywords: congenital heart disease; congenital bicuspid aortic valve; human genetics; functional genomics; TBX20; biochemical assay

 doi:10.20944/preprints202502.1131.v1

Article

Chromosomal Location and Identification of *TBX20* as a New Gene Responsible for Familial Bicuspid Aortic Valve

Yan-Jie Li [1,†], Su Zou [2,†], Yi-Zhe Bian [2], Xing-Yuan Liu [3], Chen-Xi Yang [2], Li Li [4], Xing-Biao Qiu [1], Ying-Jia Xu [2], Yi-Qing Yang [2,5,6,*] and Ri-Tai Huang [7,*]

[1] Department of Cardiology, Shanghai Chest Hospital, Shanghai Jiao Tong University School of Medicine, Shanghai 200030, China
[2] Department of Cardiology, Shanghai Fifth People's Hospital, Fudan University, Shanghai 200240, China
[3] Department of Pediatrics, Tongji Hospital, Tongji University School of Medicine, Shanghai 200065, China
[4] Key Laboratory of Arrhythmias, Ministry of Education of China, Tongji University School of Medicine, Shanghai 200092, China
[5] Cardiovascular Research Laboratory, Shanghai Fifth People's Hospital, Fudan University, Shanghai 200240, China
[6] Central Laboratory, Shanghai Fifth People's Hospital, Fudan University, Shanghai 200240, China
[7] Department of Cardiovascular Surgery, Renji Hospital, Shanghai Jiao Tong University School of Medicine, Shanghai 200127, China
* Correspondence: yangyiqing@fudan.edu.cn (Y.-Q.Y.); huangritai@renji.com (R.-T.H.); Tel.: +86-21-24289657 (Y.-Q.Y.); +86-21-68383647 (R.-T.H.)
† Contributed equally to this work.

Abstract: Congenital bicuspid aortic valve (BAV) signifies the most frequent category of congenital cardiovascular anomaly globally, occurring in approximately 0.5%–2% of the general population worldwide. BAV is a major cause of thoracic aortopathy, encompassing aortic stenosis, aortic root dilation with regurgitation, aortic dissection, and aortic aneurysms, consequently leading to substantial late-onset morbidity and mortality. Accumulating evidence convincingly demonstrates the strong genetic basis underpinning BAV, though the inheritable ingredients responsible for BAV in most patients remain largely obscure. Here, by the way of genome-wide genotyping with genetic markers, genetic linkage assay, and haplotype analysis in a multigenerational BAV family, a novel BAV-causative locus was mapped to chromosome 7p14. Sequencing assay of the genes within the mapped chromosomal region (locus) unveiled that only the c.656T>G (p.Ile219Arg) variation of *TBX20* was in co-segregation with BAV in the entire pedigree. The missense mutation was not uncovered in 322 healthy persons employed as control individuals. Functional deciphers revealed that the mutation significantly decreased the transcriptional activation of the representative target gene *ANP* and the binding ability to the *ANP* promoter and impaired the intranuclear distribution of TBX20. This investigation maps a new genetic locus (chromosome 7p14) linked to BAV and uncovers *TBX20* as a novel causative gene for familial BAV, adding more insight into the mechanisms underlying BAV and providing a molecular target for the individualized management of BAV.

Keywords: congenital heart disease; congenital bicuspid aortic valve; human genetics; functional genomics; TBX20; biochemical assay

 doi:10.20944/preprints202502.1131.v1

1. Introduction

Congenital bicuspid aortic valve (BAV) signifies the most frequently occurring form of cardiovascular developmental malformation in humans worldwide, with an overall prevalence of approximately 0.5%–2% in the general population globally [1,2]. Congenital BAV can occur as an isolated aberration or concur with other distinct types of congenital heart disease (CHD), such as atrial septal defect (ASD), aortic coarctation/stenosis, patent ductus arteriosus, pulmonary stenosis, ventricular septal defect, and endocardial cushion defect [1]. In patients with other types of CHD, the prevalence of BAV is much higher, as indicated by an example that in patients with severe aortic stenosis requiring surgery, the prevalence of BAV is as high as 50% [2]. Although BAV is frequently diagnosed by echocardiographic imaging in asymptomatic patients, approximately 33% of BAV patients suffer from severe thoracic aortic complications/valvulo-aortopathy during lifespan, including aortic valve stenosis, aortic dissection, aortic root dilation with regurgitation, and aortic aneurysm as well as bacterial endocarditis, cardioembolic cerebral stroke, ventricular fibrosis, hypoplastic left ventricle, retinal infarction, cardiac dysrhythmias, heart failure, and even premature cardiac demise [1,3–10]. It has been reported that BAV is accountable for aortic stenosis in about 70% to 85% of pediatric patients and over 50% of adult patients [10]. Moreover, aortic dilatation is detected in 30% to 70% of BAV patients, and a dysfunctional aortic valve is observed in up to 47% of BAV cases [10]. BAV also confers an 8-fold enhanced risk for aortic dissection, and the BAV-increased risks for aortic aneurysm occurrence, aortic valve replacement, and aortic surgery are 26%, 53%, and 25%, respectively, over 25 years [10]. It was reported that in the US in 2017, the aortic valve disease was accountable for about 60% of the overall deaths caused by valvular heart disease [11]. At present, trans-catheter interventional or surgical replacement of aortic valves remains the only durable treatment option, with no effective pharmacological therapies available for BAV [11,12]. Consequently, BAV leads to substantial late-onset/long-term morbidity as well as mortality, posing an enormous socioeconomic encumbrance [11,13–15]. Despite the pronounced clinical importance, the causes leading to BAV and the pathological mechanisms underpinning BAV remain largely elusive.

During embryogenesis, the heart begins to form as a single heart tube comprising an outer layer of the myocardium and an inner lining of the endocardium [16]. These two layers of the myocardia are separated by cardiac jelly, a thick hydrophilic region produced by cardiomyocytes, full of extracellular matrix, proteoglycans, glycosaminoglycans, and hyaluronic acid [16]. In the cardiac jelly, the primitive cardiomyocytes secrete some factors that drive the transition of endothelial cells into mesenchymal cells (a biological process known as endothelial-to-mesenchymal transition, namely EMT), resulting in the invasion of mesenchymal cells into the cardiac jelly [16]. In the cardiac outflow tract, EMT contributes to the formation of a parietal and a septal cushion, the primordia of the semilunar valves (aorta/pulmonary artery valves), and the septum of the outflow tract [16]. The other sources of mesenchymal cells, which are also involved in populating the endocardial cushions, originate from neural crest cells, epicardial cells, and the cells stemming from the second heart field (SHF) [1,16]. In the aortic valve, the parietal cushion (endothelial/neural crest-originated) develops into the right coronary cusp/leaflet; the septal cushion (endothelial/neural crest-originated) gives rise to the left coronary cusp/leaflet; while the non-coronary cusp/leaflet derives solely from the intercalated cushion (endothelial/neural crest/SHF-originated) on the posterior side of the outflow tract [1,16]. The normal development of endocardial cushions, the precursors of mature heart valves, is essential for proper valvular morphogenesis, and so either a failure of EMT or a defect in the contributing cell lineages (especially in cellular proliferation, specification, differentiation, migration, adhesion as well as apoptosis) may lead to aberrant aortic valvulogenesis and the pathogenesis of BAV (abnormal fusion of two aortic valve leaflets), mainly due to decreased mesenchyme populations in the endocardial cushions [1,10,11,16].

Now it is generally understood that normal aortic valvulogenesis undergoes a complicated biological process, including the formation and elongation of the endocardial cushion and the structural remodeling of the valvular cusps or leaflets, and any pathogenic factor that disturbs this

 doi:10.20944/preprints202502.1131.v1

complex developmental process may result in abnormal aortic valvular morphogenesis, including BAV [1,10,11,16,17]. Aggregating genetic investigations have demonstrated that congenital BAV is an inherited disorder, with a prevalence of roughly 9% in the first-degree relatives of BAV patients and up to 24% in those of larger BAV families [1,10,11,18]. In addition to genomic copy number variants [19], deleterious variations in an increasing number of genes have been implicated in the pathogenesis of BAV [1,10,11,17]. To date, there has been convincing cumulative evidence that pathogenic variations in >20 genes each may give rise to a small percentage of BAV, encompassing those encoding cardiac transcription factors (GATA4-6, TBX5, NKX2.5, HOXA1, KLF13, and NR2F2), signaling molecules (NOTCH1, SMAD4, and SMAD6), extracellular matrix proteins (FBN1 and FBN2), collagen proteins (COL1A2 and COL1A1), metalloproteinases (MMP9, ADAMTS5, ADAMTS16, and ADAMTS19), E3 ubiquitin ligase (MIB1), filamin A (FLNA), roundabout receptor proteins (ROBO4 and ROBO1), myosin heavy chain 6 (MYH6), mucin 4 (MUC4), palmdelphin (PALMD), protocadherin alpha 9 (PCDHA9), and cilia proteins (EXOC8, EXOC6, and EXOC4) [1,10,11,17,20–24]. Nevertheless, rare genetic variants in these established BAV-causative genes can merely explain a tiny minority of BAV patients, and the detective genetic components accountable for the development of BAV remain to be identified in most BAV-affected individuals.

2. Materials and Methods

2.1. Enrollment and Clinical Examination of Research Participants

For this retrospective clinical investigation, a 47-member pedigree (specifically designated as Family BAV-1) spanning four generations affected with congenital BAV was discovered in a Chinese population of Han ethnicity. The members available from Family BAV-1 were recruited. In total, 322 unrelated healthy individuals with no family history of CHD were enrolled as control persons. A detailed clinical investigation of the study participants was conducted by experienced cardiologists and echocardiographers, encompassing comprehensive reviews of their personal/familial histories (minimum of 3 generations) and medical histories (including CHD diagnosed previously, trans-catheter interventional procedures, and surgical operations), comprehensive and careful physical examinations, routine laboratory tests, and transthoracic echocardiograms with color Doppler. When indicated, a contrast-enhanced cardiac computed tomographic angiography was performed. A diagnosis of BAV was made if two distinct aortic valvular leaflets were confirmed by 2-dimensional echocardiographic images and/or by the medical records of trans-catheter interventional or surgical treatment of BAV-related aortopathies [10,17]. The current research was fulfilled in compliance with the standards summarized in the Helsinki Declaration released in 1975, as revised in 2008. The research protocols used for the current investigation were approved by the medical ethics committees of the Tongji Hospital, Tongji University (ethical approval code: LL(H)-09-07) and the Shanghai Fifth People's Hospital, Fudan University (ethical approval number: 2020-086), according to the local ethical regulations and the relevant national guidelines on human research. An informed consent form was signed by the research subjects or their parents/legal guardians before recruiting the study participants for this study. Peripheral blood specimens were collected in acid–citrate–dextrose (ACD)-anti-coagulated tubes from each research subject to extract genomic DNA (gDNA).

2.2. Whole-Genome Screening with Microsatellite Markers Followed by Linkage Assay

A pan-genome scan and genotyping were implemented in the 44 living members of Family BAV-1 affected with BAV by utilizing a linkage mapping set (version 2.5; Applied Biosystems, Foster City, CA, USA), which contains a total of 400 highly polymorphic microsatellite markers (short tandem repeats), spaced across the human genome at an even density of ~9.2 cM, as described elsewhere [25–27]. With the fluorescently labeled primers, multiplex amplification of the markers-containing gDNA fragments was conducted via polymerase chain reaction (PCR) using a Taq DNA Polymerase kit (Applied Biosystems, Foster City, CA, USA) on a thermal cycler instrument (Bio-Rad, Hercules, CA, USA). The amplicons were separated through gel electrophoresis on a DNA analysis apparatus

 doi:10.20944/preprints202502.1131.v1

(Applied Biosystems, Foster City, CA, USA), following the user's manual. Allele-calling was conducted with GeneMapper (version 3.1; Applied Biosystems, Foster City, CA, USA). To search for a locus linked to BAV in the family, linkage analysis was carried out in all genotyped family members to obtain the two-point logarithm of odds (LOD) scores for every microsatellite marker as previously described [25–27]. When a 2-point LOD score (a LOD score ≥2.0) supportive of linkage to BAV was yielded for a microsatellite marker, several additional markers around the marker with evidence for linkage were applied to map the locus finely. Haplotypes of Family BAV-1 affected with BAV were constructed to display the shared chromosomal region among the pedigree members suffering from BAV and confine the recombinant borders of a chromosomal region.

2.3. Sequencing Assay of the Genes within the Located BAV Locus

As previously described [28–31], a whole-exome sequencing (WES) analysis was conducted in two members suffering from BAV (Family BAV-1: II-1 and III-2) as well as one unaffected member (Family BAV-1: III-3). *In short*, the gDNA samples from the three chosen family members of Family BAV-1 underwent exome capture with a targeted capture kit, the SureSelect Human All Exon V6 kit (Agilent Technologies, Santa Clara, CA, USA), following *the manufacturer's recommendations*. The captured DNA was subject to WES under the HiSeq4000 platform (Illumina, San Diego, CA, USA) following the *user's* manual. Read data were aligned to the referential human genome (build GRCh37/hg19) with the BWA (version 0.7.17) tool [32]. With the GATK (version 3.8.1) software [33], DNA sequence variations (single-nucleotide variations and small deletions/insertions) at the targeted regions of individual genomes were identified. The pathogenic effect of all variants was predicted with the VEP (version 99) toolset [34] and annotated with ANNOVAR (version 2015) [27]. The non-synonymous variations and splicing donor/acceptor variations underwent further analysis, including the Sanger sequencing assay of a gene harboring a pathogenic variation and a co-segregation assay in the whole BAV pedigree (Family BAV-1). After a gene carrying a BAV-causative mutation was identified in Family BAV-1, Sequence assays of the same gene were completed in 322 unrelated healthy people. For a verified deleterious variation, such databases of population genetics as SNP and gnomAD were queried to verify its novelty, as described elsewhere [27].

2.4. Preparation of Gene-Expressing Plasmids

The plasmid of TBX20-pcDNA3.1 was generated as described previously [27]. The Ile219Arg-mutant TBX20-pcDNA3.1 expression vector was yielded by mutagenesis of TBX20-pcDNA3.1 using a site-targeted mutagenesis kit (Invitrogen, Carlsbad, CA, USA) as well as a pair of primers (5′-ATCAACATGGCCATAGAATTTTGAACTCAAT-3′ and 5′-ATTGAGTTCAAAATTCTATGGCCATGTTGAT-3′), and then was validated by direct sequencing analysis. The promoter of the human atrial natriuretic peptide (ANP)-encoding gene (GenBank accession number: NC_000001.11), a 960-bp gDNA fragment (from –930 to +30, with the transcriptional start site designated as +1) of the human *ANP* gene harboring multiple consensus TBX20-binding sites, was PCR-amplified from human gDNA utilizing the Platinum™ Taq DNA Polymerase (Invitrogen, Carlsbad, CA, USA) and a specific pair of primers (5′-GCAGCTAGCTGAGGGAAACTGACTATACC-3′ and 5′-TGCCTCGAGCCTCTCTTGGCCTACGTCTG-3′). The amplicons were doubly cut with the endonucleases of *Nhe*I and *Xho*I and ligated with the pGL3-Basic vector (Promega, Madison, WI, USA) utilizing the T_4 DNA ligase to produce the *ANP* promotor-driven Firefly luciferase expression vector (ANP-luc).

2.5. Cellular Transfection with Expression Plasmids and Dual-Luciferase Activity Measurement

COS7 cells were routinely cultured and seeded into wells of a 24-well plate 24 hours before transient transfection. Cells were transfected with various expression plasmids utilizing the Lipofectamine™ 3000 Transfection Reagent (Invitrogen, Carlsbad, CA, USA). To evaluate the

 doi:10.20944/preprints202502.1131.v1

transactivation of *ANP* by TBX20, COS7 cells were transfected with 800 ng of empty pcDNA3.1 (–) or 800 ng of wild-type TBX20-pcDNA3.1 (TBX20) or 800 ng of Ile219Arg-mutant TBX20-pcDNA3.1 (Ile219Arg) or 400 ng of TBX20 plus 400 ng of (–) or 400 ng of TBX20 plus 400 ng of Ile219Arg, in the presence of 1000 ng of ANP-luc and 20 ng of pRL-TK expressing Renilla luciferase (Promega, Madison, WI, USA). Cells were collected and lysed 48 hours post-transfection. The dual-luciferase activities of cellular lysates were quantitatively measured as described previously [27,35–37].

2.6. DNA-Binding Ability of Wild-type and Ile219Arg-Mutant TBX20 Proteins

Collection of COS7 cells was completed 48 hours after transient transfection and nuclear proteins were prepared as described elsewhere [27]. The DNA-binding ability of the TBX20 protein was studied by electrophoretic mobility shift assay with the *ANP* probe. The oligonucleotides of the *ANP* probe with a TBX20-binding site were synthesized and labeled with biotin on the 5′ end. The *ANP* probes and purified wild-type or Ile219Arg-mutant TBX20 nuclear protein were incubated in the Binding Buffer (Beyotime Biotechnology, Shanghai, China) for 20 minutes. Parallel unlabeled cold probes were preincubated with purified wild-type or Ile219Arg-mutant TBX20 nuclear protein for 10 minutes. Electrophoresis was performed to fractionate the protein-DNA complexes on 6% nondenaturing polyacrylamide gels at a voltage of 100 V for one hour. Then the protein-DNA complexes were transferred to a positively charged nylon membrane (ThermoFisher Scientific, Waltham, MA, USA) at 380 mA for 30 minutes, and cross-linked by exposure to ultraviolet for 20 minutes. The interaction of TBX20 with *ANP* promoter DNA was probed using streptavidin-horseradish peroxidase conjugates and detected with an EMSA kit (Beyotime Biotechnology, Shanghai, China).

2.7. Subcellular Distribution of Wild-type and Ile219Arg-Mutant TBX20 Proteins

COS7 cells were cultivated on coverslips in a 12-well plate. When cells reached an 80% growth density on the culture plate, COS7 cells were transfected with 200 ng of empty pcDNA3.1, wilt-type TBX20-pcDNA3.1, or Ile219Arg-mutant TBX20-pcDNA3.1. Cells were fixed 48 hours after transfection using 4% paraformaldehyde and rinsed briefly in cooled phosphate buffer saline (PBS). Fixed COS7 cells were heated at 95°C in an antigen retrieval solution. Next, cells were permeabilized utilizing 0.5% Triton X-100 for 5 minutes and blockaded with 3% bovine serum albumin (BSA) for 30 minutes. Subsequently, coverslips were blocked using anti-TBX20 polyclonal antibody (ABclonal, Wuhan, Hubei Province, China) at a 1: 100 dilution in an immunohistochemical wet box overnight at 4°C. Cells were washed with PBS-Tween three times and immunostained using goat anti-rabbit Alexa-Flour 594-conjugated secondary antibody (Abcam, Shanghai, China) in the immunohistochemical wet box. The cellular nuclei were stained using 4′,6-diamidino-2-phenlindole (DAPI; Sigma-Aldrich, St. Louis, MO, USA). Images were obtained under a confocal laser-scanning fluorescence microscope (Leica Microsystems, Mannheim, Germany).

2.8. Statistical analysis

Statistical analysis was made as previously described [27]. In brief, the continuous data for the promoter activities were given as mean values with standard deviations (SD). The Student's unpaired t-test was applied when the comparison was performed between two groups. For the comparison among three or more groups, the continuous variables were analyzed by utilizing one-way analysis of variance followed by Tukey's post-hoc test. A 2-tailed p-value <0.05 indicated a significant difference.

3. Results

3.1. Clinical Characteristics of the Study Pedigree with BAV

As displayed in Figure 1, a 47-member pedigree across 4 generations with BAV (Family BAV-1) was identified, from which 44 living pedigree members were recruited, clinically investigated, and

 doi:10.20944/preprints202502.1131.v1

genotyped. Among the 44 living pedigree members, 13 had congenital BAV, encompassing 8 male members and 5 female members, with an average age of 37.77 ± 19.72 years, ranging between 10 and 69 years).

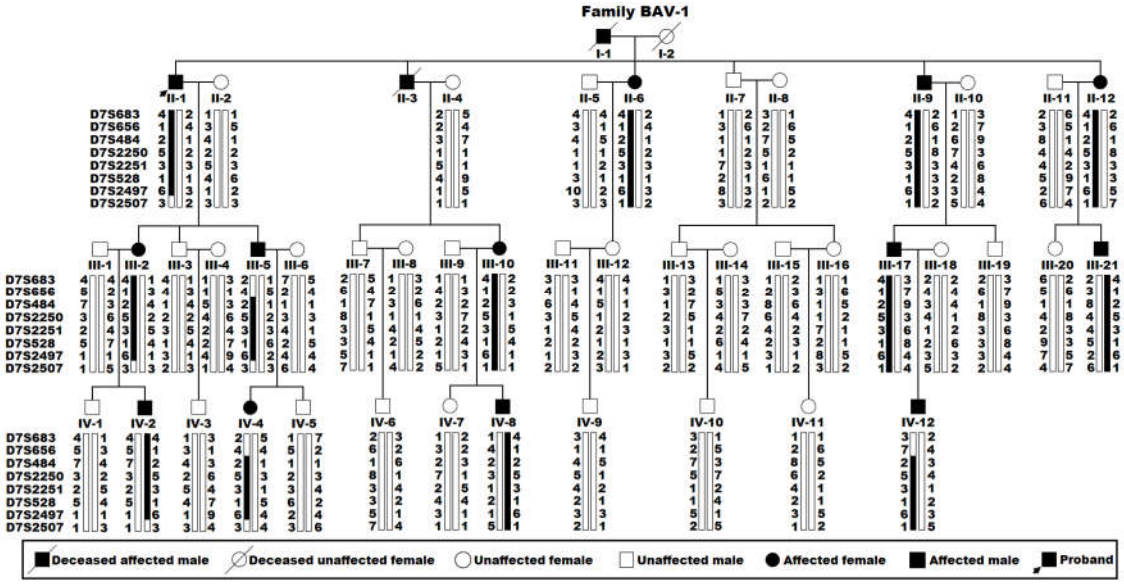

Figure 1. Haplotype analysis of a multigenerational pedigree segregating bicuspid aortic valve (BAV). An individual pedigree member is recognized by the Roman-Arabic numbers. Individual haplotypes around the *TBX20* locus were indicated by listing the allelic genotypes (symbolized with the Arabic numerals) for the chosen polymorphic genetic markers D7S683, D7S656, D7S484, D7S2250, D7S2251, D7S528, D7S2497, and D7S2507 (from top to bottom) by each individual. A vertical bar signifies the chromosomal region confined by genotype assays utilizing the selected eight markers. Blackened vertical bars indicate haplotypes segregating BAV, while open ones denote normal haplotypes. Chromosomal recombinant events in individuals II-1, III-5, and IV-12 defined the BAV locus on chromosome 7p14.1-p14.3, a chromosomal segment between marker D7S656 and marker D7S2507.

In this study pedigree (Family BAV-1), there was a total of 15 family members affected with BAV documented on their echocardiograms, including 13 living family members as shown in Table 1. The proband (Family BAV-1: II-1) was diagnosed with congenital BAV (fusion of the left and right cusps) and severe aortic valve stenosis and underwent surgical replacement of aortic valves. A representative two-dimensional echocardiogram, a color Doppler echocardiogram, and a surgical view photography of the index patient are given in Figure 2.

 doi:10.20944/preprints202502.1131.v1

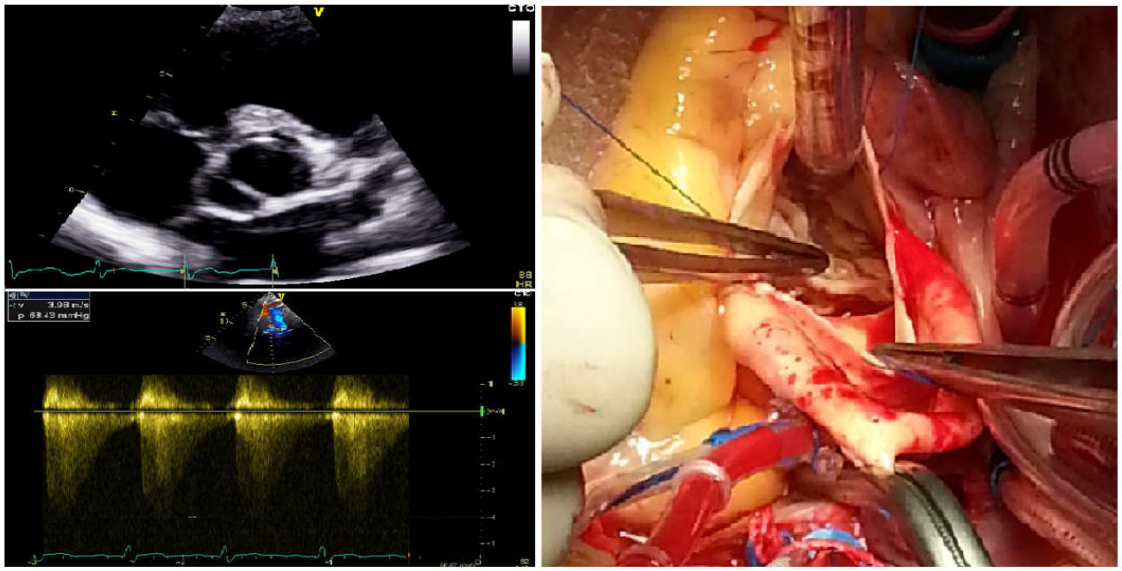

Figure 2. A representative two-dimensional echocardiogram, a color Doppler echocardiogram, and a surgical view photography of the index patient (II-1) from Family BAV-1. The representative two-dimensional echocardiogram (up left), color Doppler echocardiogram (down left), and surgical view photography (right) illustrate the bicuspid aortic valve and aortic valve stenosis.

The proband's grandfather (Family BAV-1: I-1) and younger brother (Family BAV-1: II-3) were both diagnosed with congenital BAV (fusion of the left and right cusps) and aortic valve stenosis and died of acute rupture of the aortic aneurysm and aortic dissection, respectively. Among the 13 pedigree members with congenital BAV, 3 (Family BAV-1: II-9, III-17, and IV-12) also had congenital ASD. The proband's two younger brothers (Family BAV-1: II-6, II-9) also had aortic valve stenosis. The clinical characteristic profiles and the *TBX20* genotypes of the living pedigree members affected with congenital BAV from Family BAV-1 are provided in Table 1.

Table 1. Clinical characteristic information and status of the TBX20 Ile219Arg mutation of the living pedigree members with bicuspid aortic valve from Family BAV-1.

Identity (Family BAV-1)	Sex	Ages (Years)	Phenotypes (Structural Heart Defects)	Genotypes (TBX20 Ile219Arg Mutation)
II-1	Male	69	BAV, AVS	+/–
II-6	Female	64	BAV, AVS	+/–
II-9	Male	60	BAV, AVS, ASD	+/–
II-12	Female	53	BAV	+/–
III-2	Female	45	BAV	+/–
III-5	Male	40	BAV	+/–
III-10	Female	39	BAV	+/–
III-17	Male	35	BAV, ASD	+/–
III-21	Male	23	BAV	+/–
IV-2	Male	20	BAV	+/–
IV-4	Female	17	BAV	+/–
IV-8	Male	16	BAV	+/–
IV-12	Male	10	BAV, ASD	+/–

ASD: atrial septal defect; AVS: aortic valve stenosis; BAV: bicuspid aortic valve; +/–: heterozygote.

 doi:10.20944/preprints202502.1131.v1

Additionally, a group of 322 unrelated healthy persons with no family history of CHD (197 male and 125 female persons, with a mean age of 38.16 ± 12.07 years), who were enrolled from the general population of Han ethnicity in China, were employed as control individuals. Clinical investigation revealed that all 322 control subjects had a normal cardiac structure with no BAV, as shown in their color Doppler echocardiograms.

3.2. A Novel Human BAV-linked Locus on Chromosome 7p14

A whole-genome screening with genetic markers and genetic linkage assay were completed in Family BAV-1 with congenital BAV, for the strictly defined phenotype (congenital BAV alone). In the linkage analysis for the phenotype of congenital BAV, the maximum two-point LOD score (Zmax) of 5.2802 at no recombination (recombination fraction θ = 0.00) was preliminarily obtained at marker D7S484 on chromosome 7p14, providing convincing evidence of significant linkage. To refine the BAV locus, 7 additional genetic markers (D7S683, D7S656, D7S2250, D7S2251, D7S528, D7S2497, and D7S2507) at the nearby chromosomal loci surrounding marker D7S484 were applied to genotype the living members from Family BAV-1, with a Zmax of 5.4185 at θ = 0.00 for markers D7S2250 and D7S2497, and the BAV haplotype of Family BAV-1 was deduced using the 8 genetic markers (Figure 1). Recombination events took place in one BAV-affected individual (Family BAV-1: II-1) at marker D7S2507 and two BAV-affected individuals (Family BAV-1: III-5 and IV-12) at markers D7S683 and D7S656, which defined a critical chromosomal interval for BAV, a novel familial BAV-causative locus, on chromosome 7p14 (7p14.1-p14.3; GRCh38.p14, chr7: 34,158,089–38,860,523), a ~4.62 cM (~4.70 Mb) of chromosomal interval confined by markers D7S656 and D7S2507. The LOD scores for the chosen 8 markers applied to generate the haplotype of Family BAV-1 are provided in Table 2.

Table 2. The scores of two-point logarithms of odds for the chosen eight genetic markers at chromosome 7p14.

Marker	Scores of Two-Point Logarithms of Odds at Recombination Fraction θ =						
	0.00	**0.01**	**0.05**	**0.10**	**0.20**	**0.30**	**0.40**
D7S683	(−∞)	0.7466	1.8580	2.0844	1.8682	1.2969	0.5428
D7S656	(−∞)	0.7466	1.8580	2.0844	1.8681	1.2952	0.5212
D7S484	5.2802	5.1929	4.8348	4.3654	3.3440	2.1928	0.9290
D7S2250	5.4185	5.3312	4.9730	4.5034	3.4804	2.3232	1.0247
D7S2251	2.0081	1.9710	1.8201	1.6254	1.2144	0.7774	0.3427
D7S528	4.2144	4.1446	3.8580	3.4823	2.6640	1.7400	0.7339
D7S2497	5.4185	5.3312	4.9730	4.5034	3.4804	2.3232	1.0242
D7S2507	(−∞)	1.2590	1.7430	1.7622	1.4497	0.9355	0.3356

3.3. Identification of TBX20 as a Novel Familial BAV-Causing Gene

As listed in Table A1, there are 87 known genes at the mapped chromosomal locus between D7S656 and D7S2507, including 18 genes coding for protein, 21 genes coding for non-coding RNAs, and 48 pseudogenes. Via WES and bioinformatical analysis in two pedigree members affected with BAV (Family BAV-1: II-1 and III-2) and one unaffected pedigree member (Family BAV-1: III-3) followed by Sanger sequencing analysis of *TBX20* (including all exons and splicing donors/acceptors) in all the available members from Family BAV-1, we discovered that merely the mutation c.656T>G;p.(Ile219Arg) of *TBX20* (NM_001077653.2) was linked to/in co-segregation with the BAV phenotype in the whole pedigree. The discovered *TBX20* missense mutation was neither observed in a cohort of 322 unrelated healthy people nor found in the databases of SNP and gnomAD, indicating a new mutation. The sequence electropherograms exhibiting the *TBX20* c.656T>G mutation in a heterozygous status along with its control counterpart in a homozygous status is illustrated in Figure 3.

 doi:10.20944/preprints202502.1131.v1

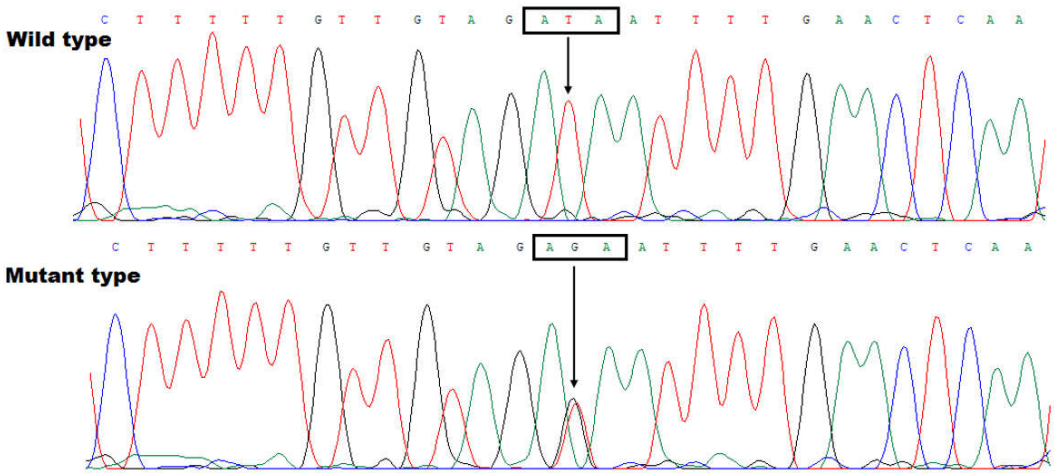

Figure 3. Sequence electropherograms exhibiting the *TBX20* c.656T>G mutation in a heterozygous status along with its control counterpart in a homozygous status. A vertical arrow points down to T/G from the proband of Family BAV-1 (mutant type) or T/T from an unaffected member of Family BAV-1 (wild type). The three nucleotides within the rectangle constitute a coding codon.

3.4. Significantly Decreased Transactivation of ANP by Ile219Arg-Mutant TBX20

As displayed in Figure 4, in contrast to wild-type TBX20 (TBX20), Ile219Arg-mutant TBX20 (Ile219Arg) had a significantly diminished transactivation of the target gene *ANP* either in a homozygous status or in a heterozygous status. Specifically, in a homozygous status, TBX20 (800 ng) and Ile219Arg (800 ng) transactivated *ANP* by ~16-fold and ~7-fold, respectively (TBX20 vs Ile219Arg: t = 8.0182, p = 0.0013); while in the heterozygous status, 400 ng of TBX20 plus 400 ng of Ile219Arg transcriptionally activated *ANP* by ~8-fold (TBX20 vs Ile219Arg + TBX20: t = 7.0462, p = 0.0059). Similar results were generated (F = 60.9672, $p = 5.503\times10^{-7}$) when the comparison was conducted among multiple groups. Specifically, for (-) vs TBX20: t = 15.0167, $p = 2.228\times10^{-7}$; for (-) vs Ile219Arg: t = 5.9867, p = 0.0008; for (-) vs TBX20 + (-): t = 8.5700, $p < 0.0001$; for (-) vs Ile219Arg + TBX20: t = 6.8533, p = 0.0003; for TBX20 vs Ile219Arg: t = 9.0300, p = < 0.0001; for TBX20 vs TBX20 + (-): t = 6.4467, p = 0.0005; for TBX20 vs Ile219Arg + TBX20: t = 8.1633, p = 0.0001; for Ile219Arg vs TBX20 + (-): t = 2.5833, p = 0.1345; for Ile219Arg vs Ile219Arg + TBX20: t = 0.8667, p = 0.8953; and for TBX20 + (-) vs Ile219Arg + TBX20: t = 1.7167, p = 0.4454.

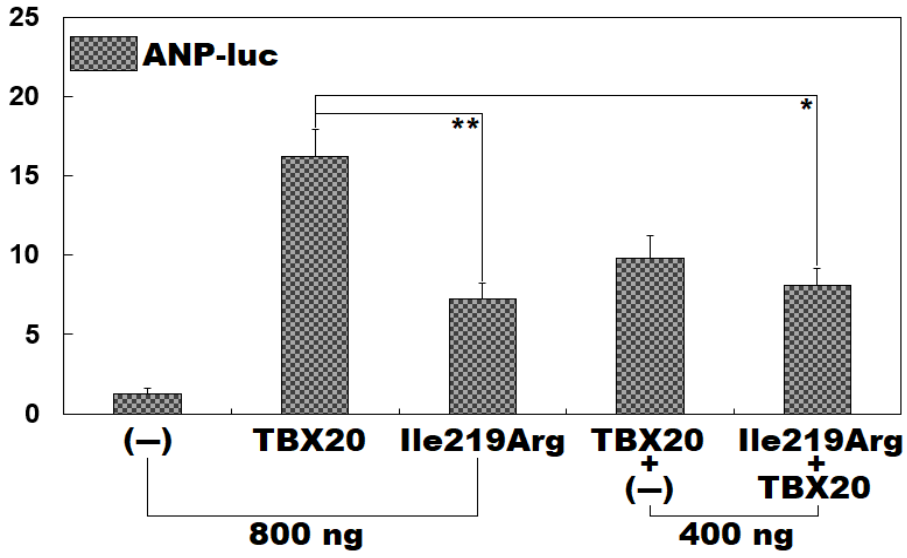

Figure 4. Reduced transactivation of *ANP* by Ile219Arg-mutant TBX20. In vitro in cultivated COS7 cells transfected with various expression vectors, a quantitative dual-luciferase activity measurement indicated that

 doi:10.20944/preprints202502.1131.v1

Ile219Arg-mutant TBX20 conferred a significantly diminished transactivation of *ANP*. A dual-reporter gene measurement was implemented three times in triplicate for each expression vector. Here, ** indicates $p < 0.005$ and * indicates $p < 0.01$, in comparison with TBX20 (800 ng).

3.5. Decreased Binding-Ability of Ile219Arg-Mutant TBX20 to the ANP Promoter

As presented in Figure 5, electrophoretic mobility shift assays indicated that the nuclear extracts of the COS7 cells expressing wild-type human TBX20 (TBX20) could interact properly with the *ANP* promoter probe to generate normal DNA-TBX20 complexes. In contrast to that of TBX20, the binding-ability of Ile219Arg-mutant human TBX20 (Ile219Arg) to the *ANP* promoter DNA probe was significantly reduced.

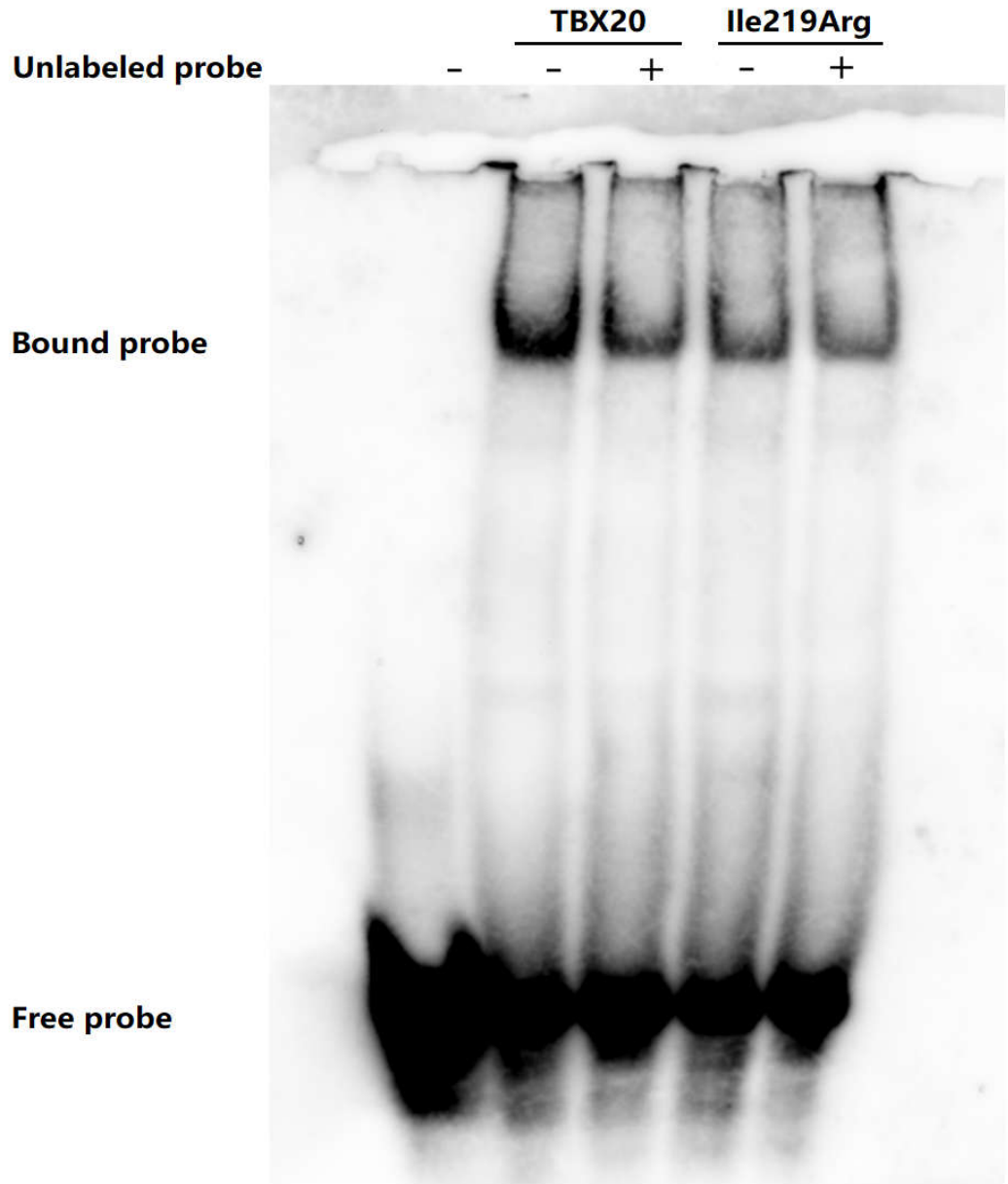

Figure 5. Significantly decreased binding-ability of Ile219Arg-mutant TBX20 to the *ANP* promoter. Wild-type human TBX20 (TBX20) could properly bind to the *ANP* promoter, whereas the DNA-binding ability of Ile219Arg-mutant human TBX20 (Ile219Arg) to the *ANP* promoter was significantly reduced.

 doi:10.20944/preprints202502.1131.v1

3.6. Abnormal Subcellular Localization of Ile219Arg-Mutant TBX20

As exhibited in Figure 6, wild-type human TBX20 (TBX20) was normally localized predominantly within the cellular nucleus. Unlike TBX20, Ile219Arg-mutant human TBX20 (Ile219Arg) showed an abnormal subcellular localization, with a major distribution to the cytoplasm rather than the cellular nucleus.

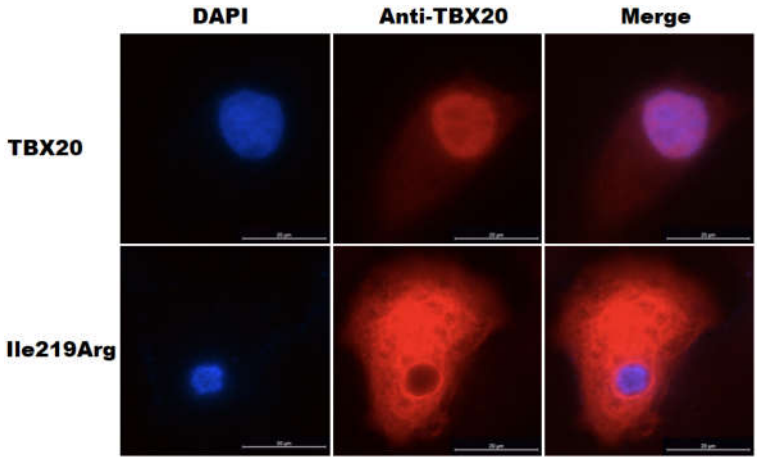

Figure 6. Abnormal intracellular localization of Ile219Arg-mutant TBX20. Subcellular localization of wild-type human TBX20 (TBX20) and Ile219Arg-mutant human TBX20 (Ile219Arg) in cultured COS7 cells was observed under a confocal fluorescence microscope. The COS7 cells expressing TBX20 or Ile219Arg were stained using anti-TBX20 and DAPI. The magnified cellular fluorescent images showed that unlikeTBX20 Ile219Arg had an abnormal subcellular distribution, predominantly in the cytoplasm rather than the cellular nuclei.

4. Discussion

In the current research, a new locus linked to congenital BAV was located at human chromosome 7p14 by a genome-wide screening with microsatellite markers, linkage assays, and haplotype ascertainments in a pedigree affected with congenital BAV. A WES analysis followed by a Sanger sequencing examination uncovered that, with the located BAV-causing locus, only the *TBX20* c.656T>G (p.Ile219Arg) mutation was in co-segregation with the BAV phenotype in the entire pedigree (Family BAV-1). The missense *TBX20* mutation was absent from the 322 healthy subjects employed as controls and was not released from the databases of SNP and gnomAD. Biochemical analyses unraveled that Ile219Arg-mutant TBX20 had a significantly diminished transactivation of its representative target gene *ANP* and reduced DNA-binding ability to the promoter of *ANP*, which might be attributed at least in part to decreased nuclear distribution of total TBX20 proteins. Hence, these results map a new familial BAV-causative locus at human chromosome 7p14 and suggest that genetically defective *TBX20* predisposes to congenital BAV.

The *TBX20* gene, which belongs to an important member of an ancient T-Box gene superfamily, maps to human chromosome 7p14-p15, encoding a transcription factor protein that consists of 447 amino acids [27,38] During embryogenesis, ample expression of TBX20 is observed in the heart throughout evolution from arthropod to vertebrate, and in almost all cardiogenic cell lineages from both cardiogenic heart fields, indicating that TBX20 serves as a key player in regulating the proper development of cardiovascular system [38–45]. Importantly, recent investigations have substantiated that TBX20 exerts a fundamental role in normal heart valve development [46-50]. In the endocardial cushion cells cultured in vitro, overexpression of *TBX20* was associated with increased cushion mesenchyme proliferation, augmented expression of MMP13 and MMP9, and decreased chondroitin sulfate proteoglycans, encompassing versican and aggrecan; in contrast, knockdown of *TBX20* was associated with decreased cushion mesenchyme proliferation, lessened expression of MMP13 and MMP9, and increased chondroitin sulfate proteoglycans, supporting that during embryogenesis

 doi:10.20944/preprints202502.1131.v1

TBX20 has a key role in mediating cell proliferation and extracellular matrix remodeling in the precursor populations of mesenchymal valve in endocardial cushions [46]. In addition, treatment with BMP2 increased the expression of TBX20 in the cells from endocardial cushions, and lack of TBX20 enhanced the expression of TBX2 and diminished the expression of NMYC1 [46]. In mice, deletion of *Tbx20* in the cardiac atrioventricular canal myocardium led to failure in the constriction of the atrioventricular canal, and the endocardial EMT was severely perturbed [47]. In addition, in the atrioventricular canal myocardium, *Tbx20* was demonstrated to have a role in maintaining the expression and function of multiple genes, including *Bmp2* and *Tbx3*, and the *Bmp2* downstream genes related to the initiation of EMT were also downregulated [47]. Furthermore, the re-expression of *Bmp2* in the myocardium of the atrioventricular canal substantially rescued the defects of EMT caused by the lack of *Tbx20*, indicating that *Bmp2* is one of the key target genes of TBX20 in the development of the cardiac atrioventricular canal [47]. Additionally, *Tbx20* has been defined as a direct transcriptional target of the BMP/SMAD (BMP2/SMAD1) signaling pathway, exerting a pivotal role in the normal morphogenesis of the atrioventricular canal and outflow tract [48,49]. On the other hand, TBX20 was found to directly interfere with the Bmp/Smad signaling pathway to suppress the expression of TBX2 in the developing chambers, thereby confining the expression of TBX2 to the region of the atrioventricular canal [50]. Moreover, TBX20 was verified to be highly expressed in the heart valves and endocardial cushions throughout cardiac organogenesis and in mice, knockout of *Tbx20* in endocardial cells led to severe defects in valve elongation and maturation (mainly due to aberrant endocardial cell proliferation and extracellular matrix development in valves), impaired cardiac function, and abnormal Wnt/β-catenin signaling pathway in the endocardial cushions [51]. Collectively, these findings demonstrate that TBX20 plays a wide variety of fundamental roles in cardiovascular development, especially in cardiac valvular morphogenesis, and genetically compromised *TBX20* predisposes to anomalous cardiac valvulogenesis, including BAV.

Previous multiple investigations have validated that TBX20 transactivates the expression of a wide variety of downstream target genes expressed abundantly in the heart, encompassing *ANP*, *KCNH2*, *GJC1*, and *GJA5*, alone or synergistically with transcriptionally cooperative partners, encompassing NKX2.5, GATA5, GATA4, and TBX5 [27,52–54], and malicious variations in the genes of *NKX2.5* [55], *GATA5* [56–59], *GATA4* [60,61], and *TBX5* [62] have been implicated with the pathogenesis of congenital BAV in humans. In this research, a new *TBX20* mutation was discovered to be accountable for familial BAV. These observational results provide genetic evidence favoring that dysfunctional *TBX20* contributes to BAV, presumably by decreasing the expression of several key target genes.

Recently, *TBX20* variations have been involved in sporadic congenital BAV [63]. Luyckx and colleagues [63] performed a rare variation burden assay utilizing the sequence data of 637 cases affected with congenital BAV/thoracic aortic aneurysm for two (*TBX20* and *DGCR6*) of the seven candidate genes carrying initially verified copy number variations (duplications and/or deletions), which revealed a suggestive genetic role for*TBX20* in the etiology for BAV/TAA. As a result, four rare deleterious *TBX20* variants were identified in the seven unrelated patients with congenital BAV/thoracic aortic aneurysm, including p.Ile39Met (c.117C>G) in one patient, p.Ser125* (c.374C>A) in one patient, p.Asp176Ala (c.527A>C) in four unrelated patients, and p.Pro178Leu (c.533C>T) in one patient. Except for p.Pro178Leu (c.533C>T), the other three *TBX20* variants were absent from the gnomAD database [63]. This study suggests that deleterious *TBX20* variants predispose to BAV/thoracic aortic aneurysm, though the functional effects of these variations remain to be expounded.

The crucial role of *TBX20* in the pathogenesis of CHD has been extensively explored [64–74]. In 2007, Kirk and coworkers [64] first reported two missense mutations and one nonsense mutation in *TBX20* identified in patients suffering from diverse cardiac pathologies, encompassing defects of septation (atrial/ventricular septal defect) and valvular malformation (mitral valve stenosis and prolapse), aortic coarctation, and cardiomyopathy [64] Subsequently, *TBX20* mutational screening investigations expanded the clinical phenotypic spectrum linked to deleterious*TBX20* mutations,

 doi:10.20944/preprints202502.1131.v1

including double outlet right ventricle, Fallot's tetralogy/pentalogy, patent ductus arteriosus, common atrioventricular canals, aortic coarctation, and persistent truncus arteriosus, and these investigations unveiled more *TBX20* mutations contributing to CHD [65–68]. In addition, *TBX20* mutations have been discovered to contribute to dilated cardiomyopathy and/or left ventricular noncompaction [69–75], as well as atrial fibrillation [27]. In the current investigation, in addition to congenital BAV, three patients carrying a *TBX20* loss-of-function mutation (Family BAV-1: II-9, III-17, and IV-12) also had congenital ASD. These studies highlight the integral roles of *TBX20* in normal cardiovascular morphogenesis and postnatal cardiac homeostasis as well as structural remodeling, suggesting that genetically defective *TBX20* predisposes to distinct heart diseases, including CHD, dilated cardiomyopathy, and arrhythmia.

5. Conclusions

The present investigation maps a new familial BAV-causing locus to human chromosome 7p14 and uncovers *TBX20* as a familial BAV-causative gene, adding insight into the molecular pathogenesis underlying congenital familial BAV and providing a new molecular target for the potential personalized therapies for familial BAV.

Supplementary Materials: The following supporting information can be downloaded at: www.mdpi.com/xxx/s1, Table A1: A list of all 87 genes at the human chromosomal locus between D7S656 and D7S2507.

Author Contributions: Conceptualization, Y.-J.L., Y.-Q.Y., and R.-T.H.; methodology, Y.-J.L., S.Z., Y.-Z.B., X.-Y.L., C.-X.Y., Y.-Q.Y., and R.-T.H.; software, Y.-J.L., S.Z., Y.-Z.B., L.L., Y.-Q.Y., and R.-T.H.; validation, Y.-J.L., S.Z., Y.-Z.B., X.-Y.L., C.-X.Y., Y.-Q.Y., and R.-T.H.; formal analysis, Y.-J.L., S.Z., Y.-Z.B., X.-Y.L., C.-X.Y., Y.-Q.Y., and R.-T.H.; investigation, Y.-J.L., S.Z., Y.-Z.B., X.-Y.L., C.-X.Y., L.L., X.-B.Q., Y.-J.X., Y.-Q.Y., and R.-T.H.; resources, Y.-J.L., X.-Y.L., X.-B.Q., Y.-J.X., Y.-Q.Y., and R.-T.H.; data curation, Y.-J.L., S.Z., Y.-Z.B., X.-Y.L., C.-X.Y., Y.-Q.Y., and R.-T.H.; writing—original draft preparation, Y.-J.L., S.Z., Y.-Z.B., X.-Y.L., C.-X.Y., L.L., X.-B.Q., Y.-J.X., Y.-Q.Y., and R.-T.H.; writing—review and editing, Y.-J.L., Y.-Q.Y., and R.-T.H.; visualization, Y.-J.L., Y.-Q.Y., and R.-T.H.; supervision, Y.-Q.Y. and R.-T.H.; project administration, Y.-Q.Y. and R.-T.H.; funding acquisition, Y.-J.L., Y.-Q.Y., and R.-T.H. All authors have read and agreed to the published version of the manuscript.

Funding: This research was funded by the Science and Technology Innovation Action Star Project of Shanghai, China (22YF1443000), the National Natural Science Foundation of China (81641014), and the Basic Research Project of Shanghai, China (20JC1418800).

Institutional Review Board Statement: The current investigation was implemented in strict compliance with the principles of the Declaration of Helsinki. The protocols applied to this study were approved by the medical ethics committees of Tongji Hospital, Tongji University School of Medicine, Shanghai (ethical approval code: LL(H)-09-07; date of approval: 27 July 2009), and Shanghai Fifth People's Hospital, Fudan University, Shanghai, China (ethical approval number: 2020-086; date of approval: 28 October 2020).

Informed Consent Statement: Written informed consent was provided by the adult study individuals or the legal guardians of adolescent study subjects.

Data Availability Statement: All data are provided in this manuscript along with Appendix A Table A1.

Acknowledgments: The authors thank all study participants.

Conflicts of Interest: The authors declare no conflicts of interest.

Abbreviations

ANNOVAR	Annotation of variation
ANP	Atrial natriuretic peptide
ASD	Arial septal defect
BSA	Bovine serum albumin
BWA	Burrows-Wheeler alignment
CHD	Congenital heart disease

 doi:10.20944/preprints202502.1131.v1

The following abbreviations are used in this manuscript:

DAPI	4′,6-Diamidino-2-phenlindole
DOAJ	Directory of open access journals
EMT	Endothelial-to-mesenchymal transition
GATK	Genome analysis toolkit
gDNA	Genomic DNA
gnomAD	Genome aggregation database
LD	Linear dichroism
LOD	Logarithms of odds
Luc	Luciferase
MDPI	Multidisciplinary Digital Publishing Institute
PBS	Phosphate buffer saline
PCR	Polymerase chain reaction
SD	Standard deviation
SHF	Second heart field
SNP	Single nucleotide polymorphism
TBX20	T-box 20
TLA	Three letter acronym
VEP	Variant effect predictor
WES	Whole-exome sequencing

Appendix A

Appendix A.1

Table A1. A list of all 87 genes at the human chromosomal locus between D7S656 and D7S2507.

CFAP144P1 (pseudo)	KRT8P20 (pseudo)	**AMPH**	RN7SL83P (pseudo)	TRG-AS1 (lncRNA)
TRG (pseudo)	TRGV1 (pseudo)	TRGV2 (pseudo)	TRGV3 (pseudo)	TRGV4 (pseudo)
TRGV5 (pseudo)	TRGV5P (pseudo)	TRGV6 (pseudo)	TRGV7 (pseudo)	TRGV8 (pseudo)
TRGVA (pseudo)	TRGV9 (pseudo)	LOC103689914 (pseudo)	TRGV10 (pseudo)	TRGVB (pseudo)
TRGV11 (pseudo)	TRGJP1 (pseudo)	TRGJP (pseudo)	**TARP**	TRGJ1 (pseudo)
TRGC1 (pseudo)	TRGJP2 (pseudo)	TRGJ2 (pseudo)	TRGC2 (pseudo)	**STARD3NL**
LOC105375236 (lncRNA)	**EPDR1**	**SFRP4**	**NME8**	CDCA3P1 (pseudo)
GPR141BP (pseudo)	**GPR141**	NECAP1P1 (pseudo)	**ELMO1**	LOC124900242 (pseudo)
RPS10P14 (pseudo)	RNU6-565P (pseudo)	LOC124901833 (lncRNA)	RPS17P13 (pseudo)	ELMO1-AS1 (lncRNA)
MIR1200 (miRNA)	LOC105375235 (lncRNA)	NPM1P18 (pseudo)	**AOAH**	AOAH-IT1 (lncRNA)
ANLN	**MATCAP2**	**EEPD1**	MARK2P7 (pseudo)	MARK2P13 (pseudo)
LOC101928618 (lncRNA)	LOC105375233 (lncRNA)	LOC107986734 (lncRNA)	SEPTIN7P3 (pseudo)	PPP1R14BP4 (pseudo)
LOC100419774 (pseudo)	RNU6-1085P (pseudo)	**SEPTIN7**	LOC107986783 (pseudo)	SEPTIN7-DT (lncRNA)
LOC442293 (pseudo)	LOC124901615 (lncRNA)	LINC03013 (lncRNA)	**HERPUD2**	HERPUD2-AS1 (lncRNA)
LOC101928421 (lncRNA)	LOC105375230 (lncRNA)	LOC401324 (lncRNA)	**TBX20**	DPY19L2P1 (pseudo)
S100A11P2 (pseudo)	LOC105375228 (lncRNA)	**DPY19L1**	LOC102724723 (lncRNA)	MIR548N (miRNA)
NPSR1	NPSR1-AS1 (lncRNA)	RN7SL132P (pseudo)	NCAPD2P1 (pseudo)	RPL7P31 (pseudo)

 doi:10.20944/preprints202502.1131.v1

RNU6-438P (pseudo)	**BMPER**

The genes coding for proteins are shown in bold fonts.

References

1. Odelin, G.; Faucherre, A.; Marchese, D.; Pinard, A.; Jaouadi, H.; Le Scouarnec, S.; FranceGenRef Consortium; Chiarelli, R.; Achouri, Y.; Faure, E.; et al. Variations in the poly-histidine repeat motif of HOXA1 contribute to bicuspid aortic valve in mouse and zebrafish. *Nat. Commun.* **2023**, *14*, 1543. doi: 10.1038/s41467-023-37110-x.
2. Kern, C.B. Excess Provisional Extracellular Matrix: A Common Factor in Bicuspid Aortic Valve Formation. *J. Cardiovasc. Dev. Dis.* **2021**, *8*, 92. doi: 10.3390/jcdd8080092.
3. Sanchez-Garcia, A.J.; Soule-Egea, M.; Fuentevilla-Alvarez, G.; Vargas-Alarcon, G.; Hernández-Mejia, B.I.; Martínez-Hernández, H.; Mora-Canela, S.L.; Santibanez-Escobar, F.; Ávila-Martinez, V.; Castrejón-Tellez, V.; et al. Role of miRNAs in Regulating Ascending Aortic Dilation in Bicuspid Aortic Valve Patients Operated for Aortic Stenosis. *Int. J. Mol. Sci.* **2025**, *26*, 779. doi: 10.3390/ijms26020779.
4. Antequera-González, B.; Martínez-Micaelo, N.; Sureda-Barbosa, C.; Galian-Gay, L.; Siliato-Robles, M.S.; Ligero, C.; Evangelista, A.; Alegret, J.M. Specific Multiomic Profiling in Aortic Stenosis in Bicuspid Aortic Valve Disease. *Biomedicines* **2024**, *12*, 380. doi: 10.3390/biomedicines12020380.
5. Tan, Y.; Li, Y.; Deng, W.; Zhang, R.; Zhao, R.; Abulipizi, A.; Zhang, J.; Ji, X.; Hou, Q.; Liu, T.; et al. Prognostic Implications of Left Atrial Strain in Bicuspid Aortic Valve With Chronic Aortic Regurgitation. *J Am Heart Assoc.* **2024**, *13*, e032770. doi: 10.1161/JAHA.123.032770.
6. Spaziani, G.; Bonanni, F.; Girolami, F.; Bennati, E.; Calabri, G.B.; Di Filippo, C.; Porcedda, G.; Passantino, S.; Nistri, S.; Olivotto, I.; et al. Aortic Dilatation in Pediatric Patients with Bicuspid Aortic Valve: How the Choice of Nomograms May Change Prevalence. *Diagnostics* **2023**, *13*, 1490. doi: 10.3390/diagnostics13081490.
7. Pereira, S.C.; Abrantes, A.L.; António, P.S.; Morais, P.; Sousa, C.; David, C.; Pinto, F.J.; Almeida, A.G.; Caldeira, D. Infective endocarditis risk in patients with bicuspid aortic valve: Systematic review and meta-analysis. *Int. J. Cardiol. Heart Vasc.* **2023**, *47*, 101249. doi: 10.1016/j.ijcha.2023.101249.
8. Zhang, J.; Li, X.; Tian, R.; Zong, M.; Gu, X.; Xu, F.; Chen, Y.; Li, C. Outcomes of Cerebral Embolic Protection for Bicuspid Aortic Valve Stenosis Undergoing Transcatheter Aortic Valve Replacement. *J. Am. Heart Assoc.* **2023**, *12*, e028890. doi: 10.1161/JAHA.122.028890.
9. Huntley, G.D.; Michelena, H.I.; Thaden, J.J.; Alkurashi, A.K.; Pislaru, S.V.; Pochettino, A.; Crestanello, J.A.; Maleszewski, J.J.; Brown, R.D. Jr.; Nkomo, V.T. Cerebral and Retinal Infarction in Bicuspid Aortic Valve. *J. Am. Heart Assoc.* **2023**, *12*, e028789. doi: 10.1161/JAHA.122.028789.
10. Wang, J.; Abhinav, P.; Xu, Y.J.; Li, R.G.; Zhang, M.; Qiu, X.B.; Di, R.M.; Qiao, Q.; Li, X.M.; Huang, R.T.; et al. NR2F2 loss-of-function mutation is responsible for congenital bicuspid aortic valve. *Int. J. Mol. Med.* **2019**; *43*, 1839–1846. doi: 10.3892/ijmm.2019.4087.
11. Ackah, R.L.; Yasuhara, J.; Garg, V. Genetics of aortic valve disease. *Curr. Opin. Cardiol.* **2023**, *38*, 169–178. doi: 10.1097/HCO.0000000000001028.
12. Li, H.D.; Li, W.Y.; Li, J.L.; Peng, S.Q.; Feng, Y.; Peng, Y.; Wei, J.F.; Zhao, Z.G.; Xiong, T.Y.; Ou, Y.X.; et al. Long-Term Durability of Transcatheter Aortic Valve Prostheses in Patients With Bicuspid Versus Tricuspid Aortic Valve. *J. Am. Heart Assoc.* **2024**, *13*, e035772. doi: 10.1161/JAHA.124.035772.
13. Yang, L.T.; Ye, Z.; Wajih Ullah, M.; Maleszewski, J.J.; Scott, C.G.; Padang, R.; Pislaru, S.V.; Nkomo, V.T.; Mankad, S.V.; Pellikka, P.A.; et al. Bicuspid aortic valve: long-term morbidity and mortality. *Eur. Heart J.* **2023**, *44*, 4549–4562. doi: 10.1093/eurheartj/ehad477.
14. Glotzbach, J.P.; Hanson, H.A.; Tonna, J.E.; Horns, J.J.; McCarty Allen, C.; Presson, A.P.; Griffin, C.L.; Zak, M.; Sharma, V.; Tristani-Firouzi, M.; et al. Familial Associations of Prevalence and Cause-Specific Mortality for Thoracic Aortic Disease and Bicuspid Aortic Valve in a Large-Population Database. *Circulation*. **2023**, *148*, 637–647. doi: 10.1161/CIRCULATIONAHA.122.060439.
15. Chatrath, N.; Westaby, J.; Finocchiaro, G.; Sharma, S.; Esteban, M.T.; Papadakis, M.; Sheppard, M.N. The role of the bicuspid aortic valve in sudden cardiac death-findings at cardiac autopsy. *Cardiovasc. Pathol.* **2023**, *65*, 107527. doi: 10.1016/j.carpath.2023.107527.
16. Peterson, J.C.; Chughtai, M.; Wisse, L.J.; Gittenberger-de Groot, A.C.; Feng, Q.; Goumans, M.T.H.; VanMunsteren, J.C.; Jongbloed, M.R.M.; DeRuiter, M.C. Bicuspid aortic valve formation: Nos3 mutation leads to abnormal lineage patterning of neural crest cells and the second heart field. *Dis. Model Mech.* **2018**, *11*, dmm034637. doi: 10.1242/dmm.034637.
17. Lin, Y.; Yang, Q.; Lin, X.; Liu, X; Qian, Y.; Xu, D.; Cao, N.; Han, X.; Zhu, Y.; Hu, W.; et al. Extracellular Matrix Disorganization Caused by ADAMTS16 Deficiency Leads to Bicuspid Aortic Valve With Raphe Formation. *Circulation* **2024**, *149*, 605–626. doi: 10.1161/CIRCULATIONAHA.123.065458.
18. Cripe, L.; Andelfinger, G.; Martin, L.J.; Shooner, K.; Benson, D.W. Bicuspid aortic valve is heritable. *J. Am. Coll. Cardiol.* **2004**, *44*, 138–143. doi: 10.1016/j.jacc.2004.03.050.

19. Carlisle, S.G.; Albasha, H.; Michelena, H.I.; Sabate-Rotes, A.; Bianco, L.; De Backer, J.; Mosquera, L.M.; Yetman, A.T.; Bissell, M.M.; Andreassi, M.G.; et al. Rare genomic copy number variants implicate new candidate genes for bicuspid aortic valve. *PLoS One* **2024**, *19*, e0304514. doi: 10.1371/journal.pone.0304514.
20. Siguero-Álvarez, M.; Salguero-Jiménez, A.; Grego-Bessa, J.; de la Barrera, J.; MacGrogan, D.; Prados, B.; Sánchez-Sáez, F.; Piñeiro-Sabarís, R.; Felipe-Medina, N.; Torroja, C.; et al. A Human Hereditary Cardiomyopathy Shares a Genetic Substrate With Bicuspid Aortic Valve. *Circulation* **2023**, *147*, 47–65. doi: 10.1161/CIRCULATIONAHA.121.058767.
21. Mansoorshahi, S.; Yetman, A.T.; Bissell, M.M.; Kim, Y.Y.; Michelena, H.I.; De Backer, J.; Mosquera, L.M.; Hui, D.S.; Caffarelli, A.; Andreassi, M.G.; et al. Whole-exome sequencing uncovers the genetic complexity of bicuspid aortic valve in families with early-onset complications. *Am. J. Hum. Genet.* **2024**, *111*, 2219–2231. doi: 10.1016/j.ajhg.2024.08.001.
22. Tessler, I.; Albuisson, J.; Piñeiro-Sabarís, R.; Verstraeten, A.; Kamber Kaya, H.E.; Siguero-Álvarez, M.; Goudot, G.; MacGrogan, D.; Luyckx, I.; Shpitzen, S.; et al. Novel Association of the NOTCH Pathway Regulator MIB1 Gene With the Development of Bicuspid Aortic Valve. *JAMA Cardiol.* **2023**, *8*, 721–731. doi: 10.1001/jamacardio.2023.1469.
23. Gehlen, J.; Stundl, A.; Debiec, R.; Fontana, F.; Krane, M.; Sharipova, D.; Nelson, C.P.; Al-Kassou, B.; Giel, A.S.; Sinning, J.M.; et al. Elucidation of the genetic causes of bicuspid aortic valve disease. *Cardiovasc. Res.* **2023**, 119, 857–866. doi: 10.1093/cvr/cvac099.
24. Delwarde, C.; Toquet, C.; Boureau, A.S.; Le Ruz, R.; Le Scouarnec, S.; Mérot, J.; Kyndt, F.; Bernstein, D.; Bernstein, J.A.; Aalberts, J.J.J.; et al. Filamin A heart valve disease as a genetic cause of inherited bicuspid and tricuspid aortic valve disease. *Heart* **2024**, *110*, 666–674. doi: 10.1136/heartjnl-2023-323491.
25. Chen, Y.H.; Xu, S.J.; Bendahhou, S.; Wang, X.L.; Wang, Y.; Xu, W.Y.; Jin, H.W.; Sun, H.; Su, X.Y.; Zhuang, Q.N.; et al. KCNQ1 gain-of-function mutation in familial atrial fibrillation. *Science* **2003**, *299*, 251–254. doi: 10.1126/science.1077771.
26. Li, Y.J.; Wang, J.; Ye, W.G.; Liu, X.Y.; Li, L.; Qiu, X.B.; Chen, H.; Xu, Y.J.; Yang, Y.Q.; Bai, D.; et al. Discovery of *GJC1* (Cx45) as a New Gene Underlying Congenital Heart Disease and Arrhythmias. *Biology* **2023**, *12*, 346. doi: 10.3390/biology12030346.
27. Li, N.; Li, Y.J.; Guo, X.J.; Wu, S.H.; Jiang, W.F.; Zhang, D.L.; Wang, K.W.; Li, L.; Sun, Y.M.; Xu, Y.J.; et al. Discovery of *TBX20* as a Novel Gene Underlying Atrial Fibrillation. *Biology* **2023**, *12*, 1186. doi: 10.3390/biology12091186.
28. Jiang, W.F.; Sun, Y.M.; Qiu, X.B.; Wu, S.H.; Ding, Y.Y.; Li, N.; Yang, C.X.; Xu, Y.J.; Jiang, T.B.; Yang, Y.Q. Identification and Functional Investigation of SOX4 as a Novel Gene Underpinning Familial Atrial Fibrillation. *Diagnostics* **2024**, *14*, 2376. doi: 10.3390/diagnostics14212376.
29. Khan, I.; Işık, E.B.; Mahfooz, S.; Khan, A.M.; Hatiboglu, M.A. Identification of Genetic Alterations in Rapid Progressive Glioblastoma by Use of Whole Exome Sequencing. *Diagnostics* **2023**, *13*, 1017. doi: 10.3390/diagnostics13061017.
30. Gu, J.N.; Yang, C.X.; Ding, Y.Y.; Qiao, Q.; Di, R.M.; Sun, Y.M.; Wang, J.; Yang, L.; Xu, Y.J.; Yang, Y.Q. Identification of *BMP10* as a Novel Gene Contributing to Dilated Cardiomyopathy. *Diagnostics* **2023**, *13*, 242. doi: 10.3390/diagnostics13020242.
31. Fang HH, Lee CL, Chen HJ, Chuang CK, Chiu HC, Chang YH, Tu YR, Lo YT, Lin HY, Lin SP. Whole Exome Sequencing Facilitates Early Diagnosis of Lesch-Nyhan Syndrome: A Case Series. *Diagnostics* **2024**, *14*, 2809. doi: 10.3390/diagnostics14242809.
32. Li, H.; Durbin, R. Fast and accurate short read alignment with Burrows–Wheeler transform. *Bioinformatics* **2009**, *25*, 1754–1760. doi: 10.1093/bioinformatics/btp324.
33. McKenna, A.; Hanna, M.; Banks, E.; Sivachenko, A.; Cibulskis, K.; Kernytsky, A.; Garimella, K.; Altshuler, D.; Gabriel, S.; Daly, M. The Genome Analysis Toolkit: A MapReduce framework for analyzing next-generation DNA sequencing data. *Genome Res.* **2010**, *20*, 1297–1303. doi: 10.1101/gr.107524.110.
34. McLaren, W.; Gil, L.; Hunt, S.E.; Riat, H.S.; Ritchie, G.R.; Thormann, A.; Flicek P., Cunningham F. The ensembl variant effect predictor. *Genome Biol.* **2016**, *17*, 122. doi: 10.1186/s13059-016-0974-4.
35. Che, H.; Zhang, X.; Cao, L.; Huang, W.; Lu, Q. LINC01614 Promotes Oral Squamous Cell Carcinoma by Regulating FOXC1. *Genes* **2024**, *15*, 1461. doi: 10.3390/genes15111461.
36. Yamaguchi, N.; Sakaguchi, T.; Wei, J.J.; Tazoe, Y.; Inamine, T.; Fukuda, D.; Ohnita, K.; Hirayama, T.; Isomoto, H.; Matsushima, K.; et al. The C/C Genotype of rs1231760 in *RGS2* Is a Risk Factor for the Progression of *H. pylori*-Positive Atrophic Gastritis by Increasing *RGS2* Expression. *Diagnostics* **2024**, *14*, 2563. doi: 10.3390/diagnostics14222563.
37. Becker, L.S.; Al Smadi, M.A.; Koch, H.; Abdul-Khaliq, H.; Meese, E.; Abu-Halima, M. Towards a More Comprehensive Picture of the MicroRNA-23a/b-3p Impact on Impaired Male Fertility. *Biology* **2023**, *12*, 800. doi: 10.3390/biology12060800.
38. Meins, M.; Henderson, D.J.; Bhattacharya, S.S.; Sowden, J.C. Characterization of the human TBX20 gene, a new member of the T-Box gene family closely related to the Drosophila H15 gene. *Genomics* **2000**, *67*, 317–332. doi: 10.1006/geno.2000.6249.

39. Chen, Y.; Xiao, D.; Zhang, L.; Cai, CL.; Li, B.Y.; Liu, Y. The Role of Tbx20 in Cardiovascular Development and Function. *Front. Cell Dev. Biol.* **2021**, *9*, 638542. doi: 10.3389/fcell.2021.638542.
40. Ji, Y.; Ma, Y.; Shen, J.; Ni, H.; Lu, Y.; Zhang, Y.; Ma, H.; Liu, C.; Zhao, Y.; Ding, S.; et al. TBX20 Contributes to Balancing the Differentiation of Perivascular Adipose-Derived Stem Cells to Vascular Lineages and Neointimal Hyperplasia. *Cell Dev. Biol.* **2021**, *9*, 662704. doi: 10.3389/fcell.2021.662704.
41. Tang, Y.; Aryal, S.; Geng, X.; Zhou, X.; Fast, V.G.; Zhang, J.; Lu, R.; Zhou, Y. TBX20 Improves Contractility and Mitochondrial Function During Direct Human Cardiac Reprogramming. *Circulation* **2022**, *146*, 1518–1536. doi: 10.1161/CIRCULATIONAHA.122.059713.
42. Das, S.; Mondal, A.; Dey, C.; Chakraborty, S.; Bhowmik, R.; Karmakar, S.; Sengupta, A. ER stress induces upregulation of transcription factor Tbx20 and downstream Bmp2 signaling to promote cardiomyocyte survival. *J. Biol. Chem.* **2023**, *299*, 103031. doi: 10.1016/j.jbc.2023.103031.
43. Edwards, W.; Bussey, O.K.; Conlon, F.L. The Tbx20-TLE interaction is essential for the maintenance of the second heart field. *Development* **2023**, *150*, dev201677. doi: 10.1242/dev.201677.
44. Bauzá, M.d.R.; López, A.E.; Simonin, J.A.; Cimbaro, F.S.; Scharn, A.; Castro, A.; Silvestro, C.V.; Cuniberti, L.A.; Crottogini, A.J.; Belaich, M.N.; et al. Effect of Intramyocardial Administration of Baculovirus Encoding the Transcription Factor Tbx20 in Sheep With Experimental Acute Myocardial Infarction. *J. Am. Heart Assoc.* **2024**, *13*, e031515. doi: 10.1161/JAHA.123.031515.
45. Zhang, D.; Shang, X.; Ji, Q.; Niu, L. Exploring genetic mapping and co-expression patterns to illuminate significance of Tbx20 in cardiac biology. *Transgenic Res.* **2025**, *34*, 5. doi: 10.1007/s11248-024-00423-8.
46. Shelton, E.L.; Yutzey, K.E. Tbx20 regulation of endocardial cushion cell proliferation and extracellular matrix gene expression. *Dev. Biol.* **2007**, *302*, 376–388. doi: 10.1016/j.ydbio.2006.09.047.
47. Cai, X.; Nomura-Kitabayashi, A.; Cai, W.; Yan, J.; Christoffels, V.M.; Cai, C.L. Myocardial Tbx20 regulates early atrioventricular canal formation and endocardial epithelial-mesenchymal transition via Bmp2. *Dev. Biol.* **2011**, *360*, 381–390. doi: 10.1016/j.ydbio.2011.09.023.
48. Mandel, E.M.; Kaltenbrun, E.; Callis, T.E.; Zeng, X.X.; Marques, S.R.; Yelon, D.; Wang, D.Z.; Conlon, F.L. The BMP pathway acts to directly regulate Tbx20 in the developing heart. *Development* **2010**, *137*, 1919–1929. doi: 10.1242/dev.043588.
49. Singh, R.; Kispert, A. Tbx20, Smads, and the atrioventricular canal. *Trends Cardiovasc. Med.* **2010**, *20*, 109-114. doi: 10.1016/j.tcm.2010.09.004.
50. Singh, R.; Horsthuis, T.; Farin, H.F.; Grieskamp, T.; Norden, J.; Petry, M.; Wakker, V.; Moorman, A.F.; Christoffels, V.M.; Kispert, A. Tbx20 interacts with smads to confine tbx2 expression to the atrioventricular canal. *Circ. Res.* **2009**, 105, 442–452. doi: 10.1161/CIRCRESAHA.109.196063.
51. Cai, X.; Zhang, W.; Hu, J.; Zhang, L.; Sultana, N.; Wu, B.; Cai, W.; Zhou, B.; Cai, CL. Tbx20 acts upstream of Wnt signaling to regulate endocardial cushion formation and valve remodeling during mouse cardiogenesis. *Development* **2013**, *140*, 3176–3187. doi: 10.1242/dev.092502.
52. Sakabe, N.J.; Aneas, I.; Shen, T.; Shokri, L.; Park, S.Y.; Bulyk, M.L.; Evans, S.M.; Nobrega, M.A. Dual transcriptional activator and repressor roles of TBX20 regulate adult cardiac structure and function. *Hum. Mol. Genet.* **2012**, *21*, 2194–2204. doi: 10.1093/hmg/dds034.
53. Stennard, F.A.; Costa, M.W.; Elliott, D.A.; Rankin, S.; Haast, S.J.; Lai, D.; McDonald, L.P.; Niederreither, K.; Dolle, P.; Bruneau, B.G.; et al. Cardiac T-box factor Tbx20 directly interacts with Nkx2-5, GATA4, and GATA5 in regulation of gene expression in the developing heart. *Dev. Biol.* **2003**, *262*, 206–224. doi: 10.1016/s0012-1606(03)00385-3.
54. Brown, D.D.; Martz, S.N.; Binder, O.; Goetz, S.C.; Price, B.M.; Smith, J.C.; Conlon, F.L. Tbx5 and Tbx20 act synergistically to control vertebrate heart morphogenesis. *Development* **2005**, *132*, 553–563. doi: 10.1242/dev.01596.
55. Qu, X.K.; Qiu, X.B.; Yuan, F.; Wang, J.; Zhao, C.M.; Liu, X.Y.; Zhang, X.L.; Li, R.G.; Xu, Y.J.; Hou, X.M.; et al. A novel NKX2.5 loss-of-function mutation associated with congenital bicuspid aortic valve. *Am. J. Cardiol.* **2014**, *114*, 1891–1895. doi: 10.1016/j.amjcard.2014.09.028.
56. Padang, R.; Bagnall, R.D.; Richmond, D.R.; Bannon, P.G.; Semsarian, C. Rare non-synonymous variations in the transcriptional activation domains of GATA5 in bicuspid aortic valve disease. *J. Mol. Cell. Cardiol.* **2012**, *53*, 277–281. doi: 10.1016/j.yjmcc.2012.05.009.
57. Shi, L.M.; Tao, J.W.; Qiu, X.B.; Wang, J.; Yuan, F.; Xu, L.; Liu, H.; Li, R.G.; Xu, Y.J.; Wang, Q.; et al. GATA5 loss-of-function mutations associated with congenital bicuspid aortic valve. *Int. J. Mol. Med.* **2014**, *33*, 1219–1226. doi: 10.3892/ijmm.2014.1700.
58. Bonachea, E.M.; Chang, S.W.; Zender, G.; LaHaye, S.; Fitzgerald-Butt, S.; McBride, K.L.; Garg, V. Rare GATA5 sequence variants identified in individuals with bicuspid aortic valve. *Pediatr. Res.* **2014**, *76*, 211–-216. doi: 10.1038/pr.2014.67.
59. Jaouadi, H.; Gérard, H.; Théron, A.; Collod-Béroud, G.; Collart, F.; Avierinos, J.F.; Zaffran, S. Identification of non-synonymous variations in ROBO1 and GATA5 genes in a family with bicuspid aortic valve disease. *J. Hum. Genet.* **2022**, *67*, 515–518. doi: 10.1038/s10038-022-01036-x.

 doi:10.20944/preprints202502.1131.v1

60. Yang, B.; Zhou, W.; Jiao, J.; Nielsen, J.B.; Mathis, M.R.; Heydarpour, M.; Lettre, G.; Folkersen, L.; Prakash, S.; Schurmann, C.; et al. Protein-altering and regulatory genetic variants near GATA4 implicated in bicuspid aortic valve. *Nat. Commun.* **2017**, *8*, 15481. doi: 10.1038/ncomms15481.
61. Li, R.G.; Xu, Y.J.; Wang, J.; Liu, X.Y.; Yuan, F.; Huang, R.T.; Xue, S.; Li, L.; Liu, H.; Li, Y.J.; et al. GATA4 Loss-of-Function Mutation and the Congenitally Bicuspid Aortic Valve. *Am. J. Cardiol.* **2018**, *121*, 469–474. doi: 10.1016/j.amjcard.2017.11.012.
62. Jiang, W.F.; Xu, Y.J.; Zhao, C.M.; Wang, X.H.; Qiu, X.B.; Liu, X.; Wu, S.H.; Yang, Y.Q. A novel TBX5 mutation predisposes to familial cardiac septal defects and atrial fibrillation as well as bicuspid aortic valve. *Genet. Mol. Biol.* **2020**, *43*, e20200142. doi: 10.1590/1678-4685-GMB-2020-0142.
63. Luyckx, I.; Kumar, A.A.; Reyniers, E.; Dekeyser, E.; Vanderstraeten, K.; Vandeweyer, G.; Wünnemann, F.; Preuss, C.; Mazzella, J.M.; Goudot, G.; et al. Copy number variation analysis in bicuspid aortic valve-related aortopathy identifies TBX20 as a contributing gene. *Eur. J. Hum. Genet.* **2019**, *27*, 1033–1043. doi: 10.1038/s41431-019-0364-y.
64. Kirk, E.P.; Sunde, M.; Costa, M.W.; Rankin, S.A.; Wolstein, O.; Castro, M.L.; Butler, T.L.; Hyun, C.; Guo, G.; Otway, R.; et al. Mutations in cardiac T-box factor gene TBX20 are associated with diverse cardiac pathologies, including defects of septation and valvulogenesis and cardiomyopathy. *Am. J. Hum. Genet.* **2007**, *81*, 280–291. doi: 10.1086/519530.
65. Liu, C.; Shen, A.; Li, X.; Jiao, W.; Zhang, X.; Li, Z. T-box transcription factor TBX20 mutations in Chinese patients with congenital heart disease. *Eur. J. Med. Genet.* **2008**, *51*, 580–587. doi: 10.1016/j.ejmg.2008.09.001.
66. Pan, Y.; Geng, R.; Zhou, N.; Zheng, G.F.; Zhao, H.; Wang, J.; Zhao, C.M.; Qiu, X.B.; Yang, Y.Q.; Liu, X.Y. TBX20 loss-of-function mutation contributes to double outlet right ventricle. *Int. J. Mol. Med.* **2015**, *35*, 1058–1066. doi: 10.3892/ijmm.2015.2077.
67. Huang, R.T.; Wang, J.; Xue, S.; Qiu, X.B.; Shi, H.Y.; Li, R.G.; Qu, X.K.; Yang, X.X.; Liu, H.; Li, N.; et al. TBX20 loss-of-function mutation responsible for familial tetralogy of Fallot or sporadic persistent truncus arteriosus. *Int. J. Med. Sci.* **2017**, *14*, 323–332. doi: 10.7150/ijms.17834.
68. Taha, M.; Awny, N.; Ismail, S.; Ashaat, E.A.; Senousy, M.A. Screening and evaluation of TBX20 and CITED2 mutations in children with congenital cardiac septal defects: Correlation with cardiac troponin T and caspase-3. *Gene* **2023**, *882*, 147660. doi: 10.1016/j.gene.2023.147660.
69. Qian L.; Mohapatra B.; Akasaka T.; Liu J.; Ocorr K.; Towbin J.A.; Bodmer R. Transcription factor neuromancer/TBX20 is required for cardiac function in Drosophila with implications for human heart disease. *Proc. Natl. Acad. Sci. U.S.A.* **2008**, *105*, 19833–19838. doi: 10.1073/pnas.0808705105.
70. Zhou Y.M.; Dai X.Y.; Huang R.T.; Xue S.; Xu Y.J.; Qiu X.B.; Yang Y.Q. A novel TBX20 loss-of-function mutation contributes to adult-onset dilated cardiomyopathy or congenital atrial septal defect. *Mol. Med. Rep.* **2016**, 14, 3307–3314. doi: 10.3892/mmr.2016.5609.
71. Zhao C.M.; Sun B.; Song H.M.; Wang J.; Xu W.J.; Jiang J.F.; Qiu X.B.; Yuan F.; Xu J.H.; Yang Y.Q. TBX20 loss-of-function mutation associated with familial dilated cardiomyopathy. *Clin. Chem. Lab. Med.* **2016**, *54*, 325–332. doi: 10.1515/cclm-2015-0328.
72. Gao, X.; Pang, S.; Ding, L.; Yan, H.; Cui, Y.; Yan, B. Genetic and functional variants of the TBX20 gene promoter in dilated cardiomyopathy. *Mol. Genet. Genomic Med.* **2024**, *12*, e2355. doi: 10.1002/mgg3.2355.
73. Amor-Salamanca, A.; Santana Rodríguez, A.; Rasoul, H.; Rodríguez-Palomares, J.F.; Moldovan, O.; Hey, T.M.; Delgado, M.G.; Cuenca, D.L.; de Castro Campos, D.; Basurte-Elorz, M.T.; et al. Role of TBX20 Truncating Variants in Dilated Cardiomyopathy and Left Ventricular Noncompaction. *Circ. Genom. Precis. Med.* **2024**, *17*, e004404. doi: 10.1161/CIRCGEN.123.004404.
74. Chang, Y.; Wacker, J.; Ingles, J.; Macciocca, I.; King, I.; Australian Genomics Cardiovascular Disorders Flagship; Semsarian, C.; McGaughran, J.; Weintraub, R.G.; Bagnall, R.D. TBX20 loss-of-function variants in families with left ventricular non-compaction cardiomyopathy. *J. Med. Genet.* **2024**, *61*, 171–175. doi: 10.1136/jmg-2023-109455.
75. Myasnikov, R.; Brodehl, A.; Meshkov, A.; Kulikova, O.; Kiseleva, A.; Pohl, G.M.; Sotnikova, E.; Divashuk, M.; Klimushina, M.; Zharikova, A.; et al. The Double Mutation DSG2-p.S363X and TBX20-p.D278X Is Associated with Left Ventricular Non-Compaction Cardiomyopathy: Case Report. *Int. J. Mol. Sci.* **2021**, *22*, 6775. doi: 10.3390/ijms22136775.